

EDGE ARTICLE

View Article Online
View Journal | View IssueCite this: *Chem. Sci.*, 2020, **11**, 10483

All publication charges for this article have been paid for by the Royal Society of Chemistry

Received 30th July 2020
Accepted 3rd September 2020
DOI: 10.1039/d0sc04183a
rsc.li/chemical-science

Introduction

Sustainable batteries using non-toxic, abundant metal anodes (Li, Na) and carbon-based cathodes are becoming increasingly viable, pushing the development of electron-accepting organic molecules to the forefront of materials research.^{1–3} Molecules that can reversibly accept multiple electrons onto a low molecular weight scaffold at high reduction potentials would allow for organic cathodes with high capacity (electrons accepted per gram) and high voltage (high reduction potential *vs.* the anode). Nevertheless, developing new acceptor scaffolds has been challenging due to the difficulty in synthesizing low molecular weight carbon-based molecules that are so highly electron-withdrawing that they can accept multiple electrons at high reduction potentials. Single-electron acceptors based off benzothiadiazole exhibit high capacity, but rather low voltages of 1–2.5 V *vs.* Li/Li⁺.⁴ Common scaffolds for organic multiple electron acceptors are viologens,^{5,6} arylene diimides,^{2,7,8} and aromatic quinones,^{9–11} which can accept two electrons between 1–3 V *vs.* Li/Li⁺. Small molecules that reversibly accept three or more electrons are difficult to find. Our group has developed

Department of Chemistry, York University, 4700 Keele Street, Toronto, ON, M3J 1P3, Canada. E-mail: tbaumgar@yorku.ca

† Electronic supplementary information (ESI) available: Experimental procedures, materials, equipment, additional electrochemical characterization of **PVS** and **PVM**, battery characterization, optical absorbance of unreduced **PVS** and **PVM**, calculated energy levels for all redox states of **PVS** and **PVM** and their Cartesian coordinates, EPR simulation parameters, and excitation energies, ¹H-NMR, ¹³C-¹H-NMR, ¹⁹F-¹H-NMR, and ³¹P-¹H-NMR spectra, and single crystal X-ray crystallography data for **PVM**. CCDC 2018920. For ESI and crystallographic data in CIF or other electronic format see DOI: 10.1039/d0sc04183a

Phosphoryl- and phosphonium-bridged viologens as stable two- and three-electron acceptors for organic electrodes†

Colin R. Bridges, Andrij M. Borys, Vanessa A. Béland, Joshua R. Gaffen and Thomas Baumgartner *

Low molecular weight organic molecules that can accept multiple electrons at high reduction potentials are sought after as electrode materials for high-energy sustainable batteries. To date their synthesis has been difficult, and organic scaffolds for electron donors significantly outnumber electron acceptors. Herein, we report the synthesis and electronic properties of two highly electron-deficient phosphaviologen derivatives from a phosphorus-bridged 4,4'-bipyridine and characterize their electrochemical properties. Phosphaviologen sulfide (**PVS**) and *P*-methyl phosphaviologen (**PVM**) accept two and three electrons at high reduction potentials, respectively. **PVM** can reversibly accept three electrons between 3–3.6 V *vs.* Li/Li⁺ with an equivalent molecular weight of 102 g (mol^{−1} e[−]) (262 mA h g^{−1}), making it a promising scaffold for sustainable organic electrode materials having high specific energy densities.

phosphoryl-bridged viologens (phosphaviologens) that accept two electrons at a reduction potential depending strongly on the valency and functionalization of the phosphorus center.^{12,13} Phosphaviologen-based materials have been used in high-voltage organic batteries operating between 2.8–3.2 V *vs.* Li/Li⁺.^{14,15} Herein, we show that *P*-bridged 4,4'-bipyridine can be used to synthesize phosphaviologen sulfide (**PVS**), a two-electron acceptor, and *P*-methyl phosphaviologen (**PVM**), a three electron acceptor. These novel multiple electron acceptors exhibit reversible reductions at between 3–3.6 V *vs.* Li/Li⁺. Excluding counterions, the **PVS** and **PVM** scaffolds exhibit theoretical capacities of 165 mA h g^{−1} and 262 mA h g^{−1}, respectively (86 mA h g^{−1} and 107 mA h g^{−1} including triflate counterions). **PVM** in particular was found to be a promising scaffold in Li-ion battery applications as a cathode material.

Results and discussion

PVS and **PVM** are synthesized using a divergent route starting from 3,3'-dibromo-4,4'-bipyridine, followed by a phosphole ring closing.¹³ 2,7-Diazadibenzophenylphosphole can be converted to **PVS** in a manner analogous to the synthesis of phosphaviologen oxides (**PVO**) (Fig. 1A),¹² as phosphorus is oxidized using elemental sulfur, and bipyridine is quaternized using methyl triflate. **PVS** is a dication related to **PVO**, a two-electron acceptor previously reported by our group, and is expected to accept two electrons in an analogous manner.^{16,17} The synthesis of **PVM** is less straightforward, as the reaction of 2,7-diazadibenzophenylphosphole with methyl triflate under normal conditions does not yield the *P*-methylated product, but rather solely the *N*-methylated product (see the ESI†). The highly



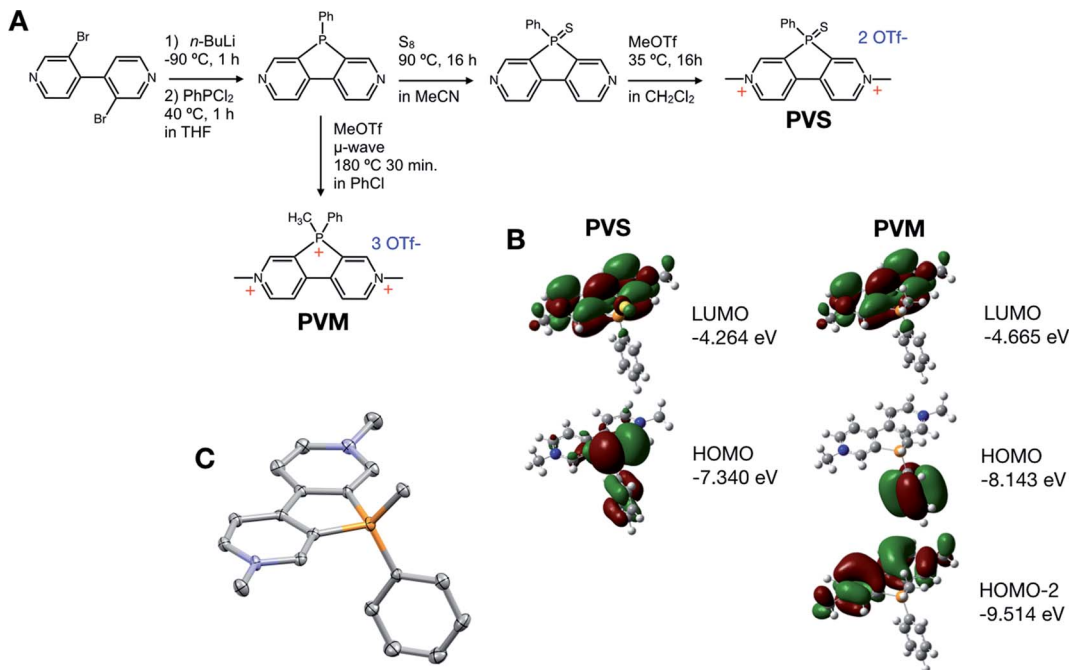


Fig. 1 (A) Synthesis of phosphoryl-bridged viologens accepting two electrons (PVS) and three electrons (PVM). (B) Relevant orbitals and energy levels. Solid-state structure for PVM (C); H atoms and anions omitted for clarity. Energy levels were calculated from optimized structures at a B3LYP/6-31+g(d) level of theory (PCM solvation applied).

electron-withdrawing nature of viologens renders the phosphorus center unreactive to even very strong electrophiles like methyl triflate. This has also been observed with dipyridinoarsoles,¹⁸ and is a common issue with the synthesis of highly electron deficient organic molecules. Only under high temperatures and pressures achieved in a microwave vial, using high boiling solvents can *P*-methylation occur to form **PVM**. **PVM** is a novel tricationic phosphoryl-bridged viologen, and theoretically accepts three electrons: two on the viologen core and one on the bridging phosphorus center. Density Functional Theory (DFT) calculations show **PVM** as a stronger electron acceptor, having lower lying HOMO and LUMO levels than **PVS**. The structure of **PVM** was also confirmed *via* single crystal X-ray crystallography, with a molecular scaffold showing planar ring systems and weak interactions towards the triflate anion (see the ESI†).

Cyclic voltammetry (CV) shows that **PVS** exhibits two one-electron reductions occurring at -0.1 V and -0.5 V *vs.* Ag/AgCl (Fig. 2A), *i.e.*, -0.6 V and -1.0 V *vs.* Fc/Fc⁺, similar to the reduction potentials of **PVO**.¹² **PVM** exhibits two reduction waves at +0.2 and -0.3 V *vs.* Ag/AgCl (-0.3 V and -0.8 V *vs.* Fc/Fc⁺), with the second reduction showing a higher peak current. Three reductions are expected, and the higher peak current indicates there are multiple reductions occurring around -0.3 V *vs.* Ag/AgCl (-0.8 V *vs.* Fc/Fc⁺). Differential pulse voltammetry (DPV) shows the second reduction wave integrates to twice the current of the first reduction wave, proving it is a two-electron redox reaction (Fig. 2B and C). We tentatively assign the first reduction in **PVM** to the quaternary phosphorus center since it occurs at a higher potential than is expected for viologens. The

reduction potentials of viologen derivatives are typically separated by 100–500 mV. In the case of **PVM**, slower scan rates and DPV could not resolve the second and third reductions, leaving them as a single peak. CV analysis of the electron-transfer rate reveals the two-electron reduction has a single, fast electron-transfer rate (see the ESI†). Viologens are known to undergo dimerization and disproportionation to form the fully reduced species from the radical cation. ^{17,19}

Some π -extended viologens, reported in the literature, also only exhibit one reduction wave for both steps (or two very closely spaced one-electron reductions), which is attributed the instability of the reduced radical cation species.²⁰ We propose that the **PVM** biradical cation rapidly disproportionates to form the triply-reduced radical and radical dication, causing the redox peaks for the second and third reduction to merge. This may be attributed to the strong propensity for biradical species to dimerize and to the higher concentration of **PVM** at the electrode surface, making dimerization more favorable compared to more dilute optical experiments (see the ESI†). Regardless of the origin of the two viologen reductions merging, **PVM** accepts three electrons, with the first reduction occurring at +0.2 V *vs.* Ag/AgCl (-0.3 V *vs.* Fc/Fc⁺) on the quaternary phosphorus and the second and third reductions occurring on the viologen core at -0.3 V *vs.* Ag/AgCl (-0.8 V *vs.* Fc/Fc⁺). These reductions occur between 3–3.6 V *vs.* Li/Li⁺ and show that **PVM** is a unique three-electron accepting scaffold. The peak to peak distance for all reductions on **PVS** and **PVM** is between 40–75 mV/n as measured by CV, indicating these reductions are highly reversible and generally suitable for battery applications (see the ESI†).



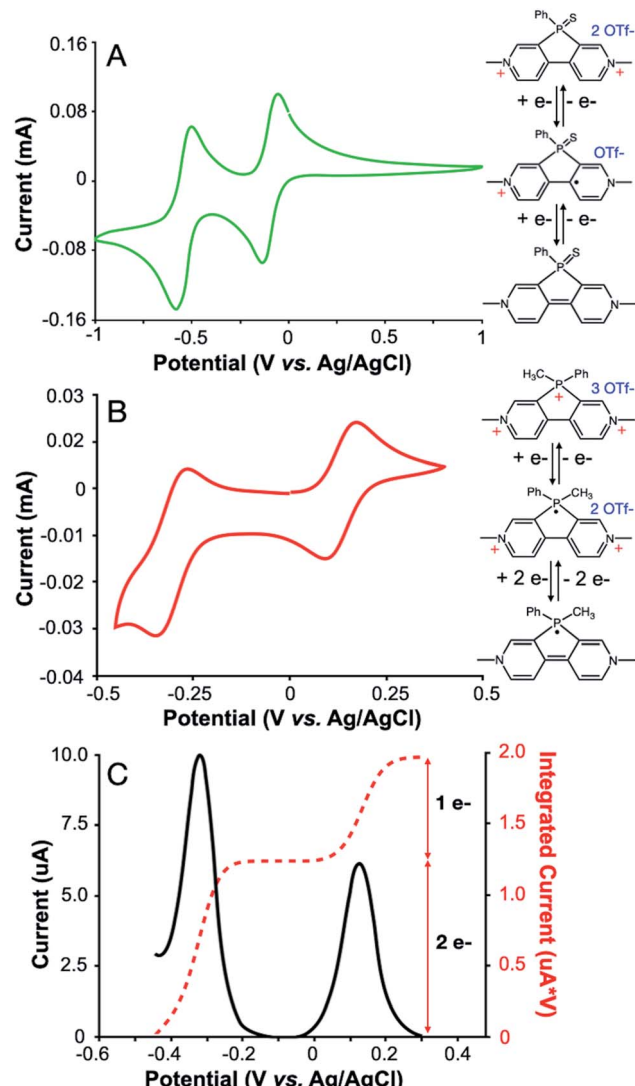


Fig. 2 (A) CV and redox reactions of PVS. (B) CV and redox reactions of PVM. (C) DPV on PVM showing the current (black) and integrated current (red) for each reduction. All experiments were conducted in a 0.1 M TBAPF₆/acetonitrile electrolyte under inert atmosphere using a glassy carbon working, Pt wire counter, and Ag/AgCl reference electrodes.

The three redox states of **PVS** and four redox states of **PVM** can be observed using chemical reductions. The colorless **PVS** dication is reduced to the radical cation using Zn powder, forming a dark blue solution. Doubly reduced neutral **PVS** is formed *via* reduction with Li metal, forming an orange solution (Fig. 3A). The colorless trication of **PVM** is converted to the singly reduced radical dication by reduction with Cu(I)Br to form a pale-yellow solution. The second and third reduction of **PVM** occur in a stepwise manner when using Zn as a reductant. The doubly reduced biradical cation is first formed, yielding a purple solution, followed by the triply reduced neutral radical to give a yellow solution (Fig. 3B). All redox species for **PVS** and **PVM** are observed using spectroelectrochemistry, exhibiting the same absorptions (see the ESI†). The high-energy absorbances

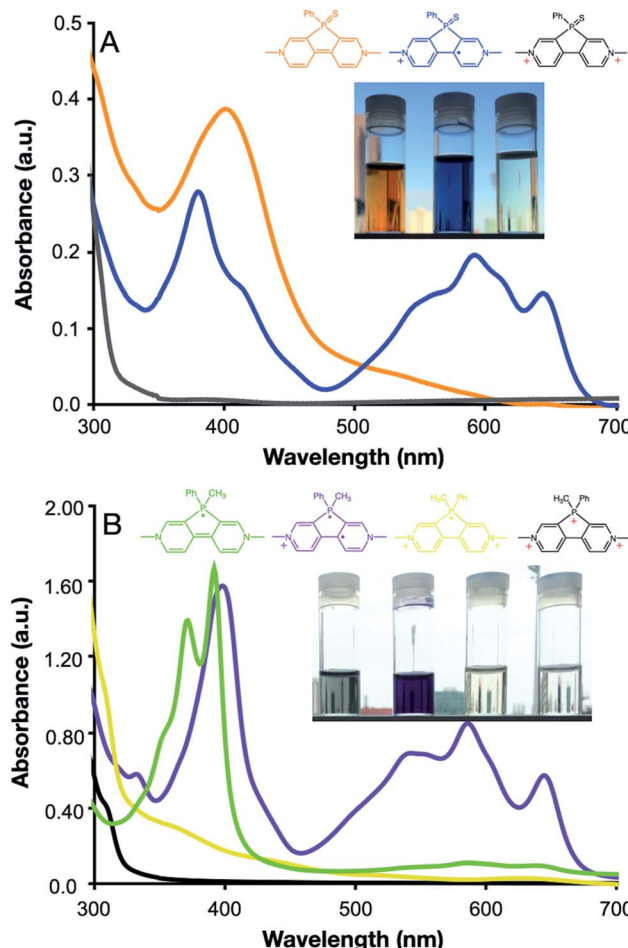


Fig. 3 (A) Optical absorbance of the various redox states of PVS isolated using chemical reductions, and photographs of their solutions (inset). (B) Optical absorbance of the various redox states of PVM isolated using chemical reductions and photos of their solutions (inset). Chemical reductions were performed in a glove box in dilute acetonitrile solutions.

of the **PVM** radical dication and neutral radical support our assignment of a localized radical centered on the phosphonium ring rather than a delocalized radical on the viologen core. TD-DFT calculations support the assignment of these radical absorptions, showing the **PVM** biradical cation and **PVS** radical cation having strong absorptions in the 600 nm range, and the **PVM** radical dication and neutral radical having strong absorptions in the 300–400 nm range (see the ESI†).

PVS exhibits one EPR spectrum for its radical cation that closely matches the splitting pattern for radical cations of phosphaviologen oxides (Fig. 4A).¹² **PVM** exhibits three distinct EPR spectra for its three radical redox states (Fig. 4B–D). In all cases, the simulated spectra closely match the experimental EPR spectra (Fig. 4). These calculations show that **PVS** holds the majority of its spin density on the viologen core, whereas **PVM** radicals show significant spin density around the phosphorus-centered ring. The radical dication and neutral radical also hold significant spin density on the phenyl and methyl functional groups on the phosphorus center, further indicating the

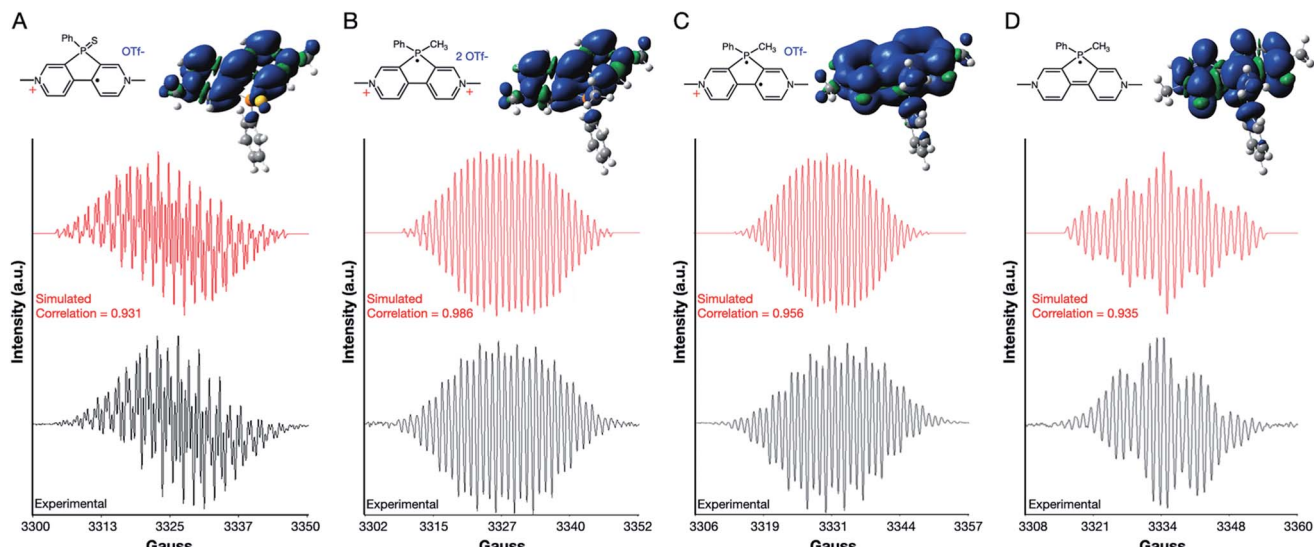


Fig. 4 Spin density maps, EPR spectra, and simulated EPR spectra for the isolated radicals of PVS (A), and PVM (B–D). Spin density maps and hyperfine coupling constants were calculated at a B3LYP/6-31+g(d) level of theory. Simulated EPR spectra were optimized using WinSim.

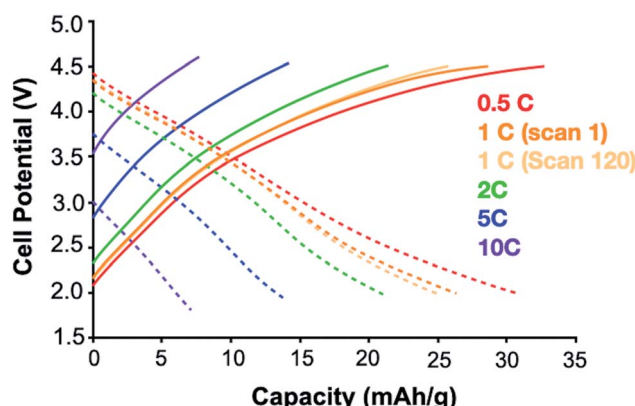


Fig. 5 Charge–discharge profiles at varying C-rates for Li-ion batteries having a PVM cathode. Coin-cell batteries were tested using a lithium reference and a saturated LiPF_6 /TEGDME electrolyte. Specific capacity is calculated including the mass of a triflate counterion.

importance of the phosphonium cation in allowing the unique tricationic viologen to stably accept three electrons (see the ESI†).

Phosphaviologen oxide (**PVO**) derivatives function as cathode in high-voltage batteries with a lithium anode, having charging and discharging plateaus between 2.8–3.2 V vs. Li/Li^+ .^{16,17} To explore how **PVM** functions as an organic energy-storage material we fabricated batteries having a Li anode and **PVM** cathode (which would correspond to a dual-ion battery type in a full cell setup).²¹ An electrolyte solution saturated in lithium triflate was used to minimize the solubility of **PVM** via the common ion effect. The battery was charged and discharged between 2–4.5 V vs. Li/Li^+ at various scan rates, showing moderate shoulders between 3–4 V vs. Li/Li^+ due to the redox reactions of **PVM** (Fig. 5). The cell exhibited good cycle stability, with negligible capacity fading after 120 charge/discharge cycles. The observed capacity is only roughly 30% of the

theoretical capacity, indicating most of the electrode material is dissolved in the electrolyte solution.¹⁵ While this result is somewhat disappointing it nevertheless provides an important proof-of-concept for the utility of **PVM** as a high voltage cathode material. Alternative synthetic strategies to reduce the solubility of **PVM** are currently being explored to allow the intrinsic high voltage and high capacity of these novel materials to be achieved.

Conclusions

In conclusion, we have synthesized two new small multiple-electron acceptor molecules having high reduction potentials versus Li, a common battery anode metal. **PVS** accepts two electrons delocalized across the viologen core, while **PVM** accepts one electron localized on the phosphorus-centered ring, and two additional electrons delocalized across the viologen core between 3.0–3.6 V vs. Li/Li^+ . **PVM** is a particularly promising energy-storage material being a rare example of a small molecule able to accept three electrons at high voltages vs. Li/Li^+ . Li-ion batteries fabricated using **PVM** as the cathode exhibit a high voltage, but the high solubility of **PVM** decreases the overall capacity and lifetime of the battery. Efforts to modify the **PVM** scaffold to reduce its solubility are ongoing.

Conflicts of interest

There are no conflicts to declare.

Acknowledgements

Financial support by the Natural Sciences and Engineering Research Council of Canada and the Canada Foundation for Innovation is gratefully acknowledged. C. R. B. would like to



acknowledge a York Science Fellowship, and T. B. thanks the Canada Research Chairs program for support.

References

- 1 B. C. Melot and J. M. Tarascon, *Acc. Chem. Res.*, 2013, **46**, 1226–1238.
- 2 T. B. Schon, B. T. McAllister, P.-F. Li and D. S. Seferos, *Chem. Soc. Rev.*, 2016, **45**, 6345–6406.
- 3 S. Muench, A. Wild, C. Fribe, B. Häupler, T. Janoschka and U. S. Schubert, *Chem. Rev.*, 2016, **116**, 9438–9484.
- 4 L. Chen, C. R. Bridges, G. Gao, T. Baumgartner and X. He, *ACS Appl. Energy Mater.*, 2019, **2**, 7315–7320.
- 5 G. Li, B. Zhang, J. Wang, H. Zhao, W. Ma, L. Xu, W. Zhang, K. Zhou, Y. Du and G. He, *Angew. Chem., Int. Ed.*, 2019, **58**, 8468–8473.
- 6 A. Jouhara, E. Quarez, F. Dolhem, M. Armand, N. Dupré and P. Poizot, *Angew. Chem., Int. Ed.*, 2019, **58**, 15680–15684.
- 7 H. Wang, S. Yuan, D. Ma, X. Huang, F.-L. Meng and X.-B. Zhang, *Adv. Energy Mater.*, 2014, **4**, 1301651–1301657.
- 8 A. Iordache, V. Delhorbe, M. Bardet, L. Dubois, T. Gutel and L. Picard, *ACS Appl. Mater. Interfaces*, 2016, **8**, 22762–22767.
- 9 N. Patil, A. Aqil, F. Ouhib, S. Admassie, O. Inganäs, C. Jérôme and C. Detrembleur, *Adv. Mater.*, 2017, **29**, 1703373–1703379.
- 10 H. Wu, S. A. Shevlin, Q. Meng, W. Guo, Y. Meng, K. Lu, Z. Wei and Z. Guo, *Adv. Mater.*, 2014, **26**, 3338–3343.
- 11 T. B. Schon, A. J. Tilley, C. R. Bridges, M. B. Miltenburg and D. S. Seferos, *Adv. Funct. Mater.*, 2016, **26**, 6896–6903.
- 12 M. Stolar, J. Borau-Garcia, M. Toonen and T. Baumgartner, *J. Am. Chem. Soc.*, 2015, **137**, 3366–3371.
- 13 S. Durben and T. Baumgartner, *Angew. Chem., Int. Ed.*, 2011, **50**, 7948–7952.
- 14 C. R. Bridges, M. Stolar and T. Baumgartner, *Batteries Supercaps*, 2020, **3**, 268–274.
- 15 M. Stolar, C. Reus and T. Baumgartner, *Adv. Energy Mater.*, 2016, **6**, 1600944–1600949.
- 16 L. Striepe and T. Baumgartner, *Chem.-Eur. J.*, 2017, **15**, 16924–16940.
- 17 C. L. Bird and A. T. Kuhn, *Chem. Soc. Rev.*, 1981, **10**, 49–82.
- 18 T. Fujii, S. Tanaka, S. Hayashi, H. Imoto and K. Naka, *Chem. Commun.*, 2020, **56**, 6035–6038.
- 19 J. W. Park, N. H. Choi and J. H. Kim, *J. Phys. Chem.*, 1996, **100**, 769–774.
- 20 M. E. Alberto, B. C. De Simone, S. Cospito, D. Imbardelli, L. Veltri, G. Chidichimo and N. Russo, *Chem. Phys. Lett.*, 2012, **552**, 141–145.
- 21 M. Wang and Y. Tang, *Adv. Energy Mater.*, 2018, **8**, 1703320.

